Simulation wetting and drying of mangrove forests due to tidal currents in Qeshm canal

S.R. Sabbagh-Yazdi, M. Zounemat-Kermani and N.E. Mastorakis

Abstract— The main aim of the present paper is devoted to simulate flow pattern in the Qeshm canal which is affected by two open boundary conditions at inlet and outlet of the canal, which are formed by tidal currents in the Persian Gulf. In this paper, hydrodynamic simulation of tidal currents in the Qeshm canal due to tidal fluctuations in Hurmoz Strait is presented. The mathematical model utilized consists of depth averaged equations of continuity and motion in two-dimensional horizontal plane which considering hydrostatic pressure distribution. The cell-vertex finite volume method is applied for converting the governing equations into discrete form for unstructured control volumes. In order to reduce the unwanted errors during model running, an artificial viscosity formulation, was used which is designed for the unstructured triangular meshes. The quality of the model results is verified by comparison between numerical results and reported data in the literature for flow in a channel with a spur dike. Finally, the performance of the computer model to simulate tidal flow in a geometrically complex domain, which is subject to wetting and drying is examined by simulation of tidal currents in the Qeshm canal in the Persian Gulf.

***Keywords*—** Mangrove Forest, Wetting and Drying, Finite Volume, Qeshm Canal, Persian Gulf

I. Introduction

The Qeshm canal is situated in the north-east of the Persian Gulf, which is tremendously affected by tidal currents. There are some mangrove forests in the Qeshm with magnificent landscape. Mangroves are densely vegetated mudflats that exist at the boundary of marine and terrestrial environments. In this stunning forest, the roots of mangrove trees are floated in saline water therefore, the forests are subject to wet and drying during the tidal periods. Having a better insight Fig. 1 shows a view of the forests mangrove in Qeshm canal (Persian Gulf). The flow regime in marine waterways such as the Qeshm canal has a significant effect on biological processes. The hydrodynamic modeling of tidal currents in Qeshm canal can serve as useful tool for investigation on mangrove forest from the environmental point of view. However, the concept of wet and drying makes this modeling case a challenging task.

Fig. 1, A view of Qeshm's mangrove forest

Water free surface treatment is one of the major difficulties in numerical solution of three dimensional water flow patterns. Some of the models apply a normalized coordinate (sigma coordinate) system in vertical direction to solve three dimensional flow equations. Shallow water flow solvers are models with low computational costs and suitable for the cases in which vertical component of the flow velocities are negligible [1], [2]. Several numerical models were used to simulate hydrodynamic behaviour of flow in mangrove forests [14]. Among studied researches, using 2D depth average equations in numerical modelling of mangrove forest has received a great interest [15], [16].

However, 2D numerical models should be able to account the wet and dry processes by moving boundary techniques. A variety of approaches have been utilized to represent wetting and drying in finite difference, and finite element numerical models for free surface flows [17, 18]. Furthermore, several finite volume methods utilized for wet/dry simulation [19]-[21]. A review of several approaches for the representation of the moving boundary is given by Balzano [10]. Also, Bradford and Sanders [22] varied the free surface reconstruction scheme near the wet/dry interface to prevent spurious wave generation at boundaries.

In this paper, a version of NASIR (Numerical Analyzer for Scientific and Industrial Requirements) software which is developed for finite volume solution of shallow water equations is assessed for simulation of tidal flow patterns in a canal with variable bathymetry. Therefore, the model is tested for the circulating turbulent flow and then, the efficiency of the special treatments are considered for moving coastal boundaries is examined by simulation of tidal flow in the Qeshm canal (north east of the Persian Gulf) considering the wetting and drying of its mangrove forests.

Saeed-Reza Sabbagh-Yazdi, Associate Professor of Civil Engineering Department, K.N. Toosi University of Technology, 1346 Valiasr St. Tehran, IRAN (phone: +9821-88521-644; fax: +9821-8877-9476; e-mail: SYazdi@kntu.ac.ir).

Mohammad Zounemat-Kermani, PhD candidate of Civil Engineering Department, KN.Toosi University of Technology, 1346 Valiasr St. Tehran, Iran, (e-mail: zounemat@computermail.net)

Nikos E. Mastorakis, Professor of Military Insitutes of University Education ASEI) Hellenic Naval Academy Terma Chatzikyriakou 18539, Piraues, GREECE (e-mail:mastor@wseas.org)

 Manuscript received Sept. 19, 2007; Revised received Jan. 12, 2008

II. Governing Equations

The convection-diffusion equation, which is formed by both transport and diffusion terms, is applied to model the transient depth average currents. The depth averaged equations (Shallow Water Equations) are chosen as the governing equation of the flow in the Persian Gulf. The governing equations are written in vector form as follows:

$$\frac{\partial W}{\partial t}+(\frac{\partial F^{i}}{\partial x}+\frac{\partial G^{i}}{\partial y})=(\frac{\partial F^{v}}{\partial x}+\frac{\partial G^{v}}{\partial y})+S \tag{1}$$

$$W=\begin{pmatrix} h \\ hu \\ hv \end{pmatrix},\quad F^{i}=\begin{pmatrix} hu \\ hu^{2} \\ huv \end{pmatrix},\quad G^{i}=\begin{pmatrix} hv \\ huv \\ hv^{2} \end{pmatrix} \tag{2}$$

$$F^{v}=\begin{pmatrix} 0 \\ h\nu_{th}2(\frac{\partial u}{\partial x}) \\ h\nu_{th}(\frac{\partial v}{\partial x}+\frac{\partial u}{\partial y}) \end{pmatrix} \tag{3}$$

$$G^{v}=\begin{pmatrix} 0 \\ h\nu_{th}(\frac{\partial u}{\partial y}+\frac{\partial v}{\partial x}) \\ h\nu_{th}2(\frac{\partial v}{\partial y}) \end{pmatrix} \tag{4}$$

$$S=\begin{pmatrix} q_z \\ -gh\frac{\partial \eta}{\partial x}+hvf_c-\frac{\tau_{bx}}{\rho_w}+\frac{\tau_{wx}}{\rho_w} \\ -gh\frac{\partial \eta}{\partial y}-huf_c-\frac{\tau_{by}}{\rho_w}+\frac{\tau_{wy}}{\rho_w} \end{pmatrix} \tag{5}$$

Where, W represents the conserved variables using h flow depth, u and v the horizontal components of velocity. G^{i} and F^{i} are vectors of inviscid terms (convective fluxes), while, G^{v} and F^{v} are vectors of viscous terms (diffusive fluxes) of W in x and y directions, respectively. The vector S contains the source and sinks terms of the governing equations. Also bed friction global stresses can be calculated as the following in x and y directions respectively,

$$\tau_{bx}=\rho_w C_f u|U|$$
$$\tau_{by}=\rho_w C_f v|U| \tag{6}$$

Where $C_f=gn^2/h^{1/3}$ (n represents manning coefficient). In the present work, the widely used depth-averaged parabolic turbulent model is applied, in which the eddy viscosity parameter is computed by the following algebraic formulation

$$\nu_{th}=\theta\, hU_*. \tag{7}$$

In this formulation the bed friction velocity is defined as

$$U_*=\sqrt{[C_f\,(u^2+v^2)]} \tag{8}$$

The empirical coefficient θ is advised between 0.067 to 0.2. This turbulence model is known suitable for depth averaged equations and has been used in some similar applications [3]-[5].

III. Numerical Formulations

Ignoring source terms, using finite volume would convert the governing equations into discrete form by integrating over a control volume Ω.

$$\frac{\partial}{\partial t}\int_{\Omega}W\,.d\Omega+\int_{\Omega}(\frac{\partial}{\partial x}F^{i}+\frac{\partial}{\partial y}G^{i}).d\Omega=\int_{\Omega}(\frac{\partial}{\partial x}F^{v}+\frac{\partial}{\partial y}G^{v})d\Omega \tag{9}$$

Where superscripts i denotes inviscid terms whereas superscript v stands for viscous terms. Using green's theorem, the volume integral of inviscid and viscous terms (convective and diffusive fluxes) are converted to boundary integrals as,

$$\frac{\partial}{\partial t}\int_{\Omega}W\,.d\Omega+\int_{\Gamma}(F^{i}dy-G^{i}dx).=\int_{\Gamma}(F^{v}dy-G^{v}dx) \tag{10}$$

Using the application of cell vertex (overlapping) scheme of the finite volume method, considering proper techniques to convert diffusive fluxes into discrete form and source term treatment, this method ends up with the following formulation

$$W_i^{t+\Delta t}=W_i^{t}-\frac{\Delta t}{\Omega_i}.\sum_{k=1}^{N_{sides}}[(\bar{F}^{i}\Delta y-\bar{G}^{i}\Delta x)-(\tilde{F}^{v}\Delta y-\tilde{G}^{v}\Delta x)]_k^t+\frac{\Delta t}{3}S_i^t \tag{11}$$

Where W_o represents conserved variables at the centre of control volume Ω_o. the solution domain is decomposed into a number of triangular cells, on which the flow variables are stored at the vertices. The control volume for a vertex i is defined as the union of all the triangles having a vertex at i, as shown in Fig. 2. Note that for the vertex base finite volume, there is no need to reconstruct the nodal variables from the

variables computed at the centre of the cells.

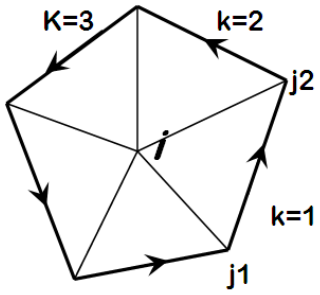

Fig. 2, A typical control volume gathered by triangles

The residual term, consists of convective and diffusive part.

$$R(W_i)=\sum_{k=1}^{N_{sides}}[(\bar{F}^i\Delta y-\bar{G}^i\Delta x)-(\tilde{F}^v\Delta y-\tilde{G}^v\Delta x)]_k^t \qquad (12)$$

In smooth parts of the flow domain, where there is no strong gradient of flow parameters, the convective part of the residual term is dominated. Since, in the explicit computation of convective dominated flow there is no mechanism to damp out the numerical oscillations, it is necessary to apply numerical techniques to overcome instabilities with minimum accuracy degradation. In the present work, the artificial dissipation terms suitable for the unstructured meshes are used to stabilize the numerical solution procedure. In order to damp unwanted numerical oscillations, a fourth order artificial dissipation term, is added to above algebraic formula.

$$D(W_i)=\varepsilon\sum_{j=1}^{N_{edges}}\lambda_{ij}(\nabla^2W_j-\nabla^2W_i) \qquad (13)$$

In which λ_{ij} is a scaling factor and is computed using the maximum value of the spectral radii of every edge connected to node i ($1/256\le\varepsilon\le 3/256$). Here, the Laplacian operator at every node *i*, $\nabla^2W_i=\sum_{j=1}^{N_{edges}}(W_j-W_i)$, is computed using the variables W at two end nodes of edges (meeting node *i*). The revised formula, which preserves the accuracy of the numerical solution, is written in the following to following relation.

$$W_i^{t+\Delta t}=W_i^t-\frac{\Delta t}{\Omega_i}.\{R(W_i^t)-D(W_i^t)\} \qquad (14)$$

Δt is the minimum time step of the domain proportional to the minimum mesh spacing and maximum wave speed of the convective homogonous equations [6]-[8].

IV. Boundary Conditions

Two major type of boundary conditions of flow and wall boundary condition considered in the current research.

A. Flow Boundary Conditions

The tidal flow boundary condition (like outer boundary of the test case) can be applied by imposing the water surface level fluctuations at tidal flow boundary. Surface water oscillating boundary condition was imposed at the inlet boundary as SHAHID-RAJAEE port (east boundary) and BASAEED port (west boundary). Regarding to the shortage of data for water level oscillation in west boundary through numerical simulation period, the simulation and prediction of water level of tides was applied by 36 tidal constituents of Iranian national cartography centre tide's poll. For achieving this data in the form water level fluctuations, harmonica analysis was used. For the east boundary, the tide gauge data of national cartography centre was applied.

B. Wall boundary Conditions

Free-slip velocity condition walls can be imposed where no flow passes through a vertical plane of the flow domain. This is the condition for straight borders of the first test case. At these boundaries the component of the velocities normal are set to zero. Therefore tangential computed velocities are kept using free slip condition at wall boundaries [9]. One of the most remarkable points about the present study is imposing proper moving boundary condition due to tidal currents. Thereafter, wetting and drying technique was implemented in the model. Next section is devoted to describe the wet/dry moving boundary process.

V. Implementing Wetting and Drying Process

In finite volume method, wetting and drying fronts are considered as moving boundaries. Considering an edge base algorithm, each edge can be considered as dry if the flow depth is below a specific value so-called critical depth on both its nodes (edge *k* in Fig. 3). In dry nodes, negative and depths less than critical depth are replaced by a prescribed depth and the velocity is assumed to be zero [4], [10]. This read as,

$$\begin{aligned} h_{Dry\ node}&=h_{cr}\\ \vec{v}_{Dry\ node}&=0 \end{aligned} \qquad (15)$$

Moreover, in the above described algorithm, the end nodes of dry edges are considered as dry points (Fig. 3). Furthermore, it is assumed that no mass and momentum fluxes pass through an edge that the water depth at it's end nodes are less than the prescribed minimum depth. This yields to the following conditions:

$$(h_L<h_{cr})\ \ and\ \ (h_R<h_{cr})\rightarrow No\ \ Flux \qquad (16)$$

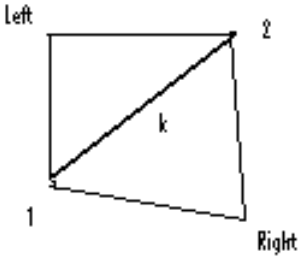

Fig. 3, representation edge k between the left and right control volumes

VI. Circulating Flow Simulation

In this section, the accuracy of the model to simulate circulating deep flow in a channel with a spur dike is assessed by comparing numerical results with the reported experimental measurements. The test case of channel with a spur dike as an obstacle is chosen for verification of the numerical model for solving the circulations in flow due to the irregularities of wall boundary [12].

The channel width is *0.915m* and has a length of 5m. The inflow and outflow boundaries are the left side right side of the channel. At the left side of the channel (inflow boundary) the mean velocity is *0.22m/s* and the flow depth is *0.223m*. The dike is placed at 0.92m distance from the inflow with 0.152m height. The channel is made by aluminium and a manning coefficient of 0.1 was chosen as the roughness of the channel.

The domain is discritized with triangular unstructured mesh, which contains 1132 nodes and 2034 cells and local mesh refinement is imposed near the spur dike (Fig. 4). Slip boundary condition is imposed on the side walls. At upstream flow boundary of the channel *x* direction velocity is imposed.

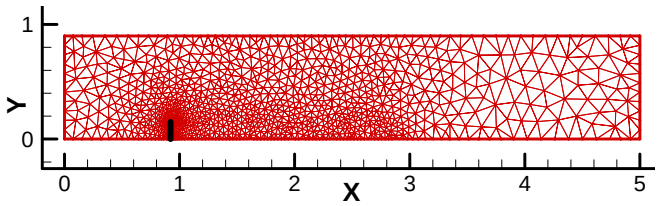

Fig. 4. The triangular mesh of the channel with spur dike

As shown in Fig. 5, streamlines circulation is formed after the spur dike. The length of recirculation region is approximately *1.95* which is close to experimental measurement of *1.80m* (which shows 8% error in computed results).

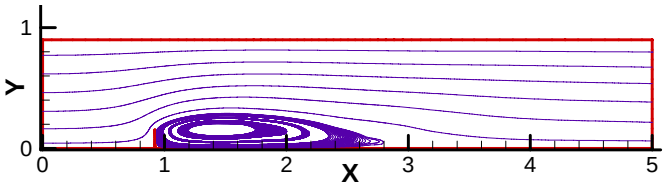

Fig. 5. Stream lines and recirculation region downstream of the side-wall expansion

VII. Wet and Dry Simulation

The Qeshm canal is placed at the top of the Qeshm Island which is located in the inlet part of the Persian Gulf next to the Hurmoz Strait. Fig. 6 shows the Qeshm Island location in the Persian Gulf.

Fig. 6 . Position of the Qeshm Island in the Persian Gulf

The coastal boundary and the bed surface topography of the Qeshm is very irregular. A numerical model is not able to simulate the real world flow pattern unless the geometrical characteristics of flow domain are modelled precisely. Thus, the numerical flow solver should handle the geometrical complexities of the bed and boundaries of the flow domain. In order to overcome the problem, attempt has made to solve the depth averaged hydrodynamic equations on unstructured finite volumes.

Application of unstructured mesh facilitates considering the effects of geometrical irregularities of coasts [13]. The three dimensional surface of flow bed is modelled in two stages. In the first stage, horizontal geometry of the problem is modelled by definition of some boundary curves, (281 curves of coastal boundaries) and then, the domain is discretized with triangular unstructured mesh which contains 3599 nodes, and 10218 cells. In the second stage, for converting the two dimensional mesh into a three dimensional surface, the bed elevation of the flow domain is digitized at a number of points along some contour lines. Then, the bed elevation is set for the every node of the mesh by interpolation of the elevations of surrounding digitized points. Fig. 7 shows the constructed coloured triangular meshes within the computational.

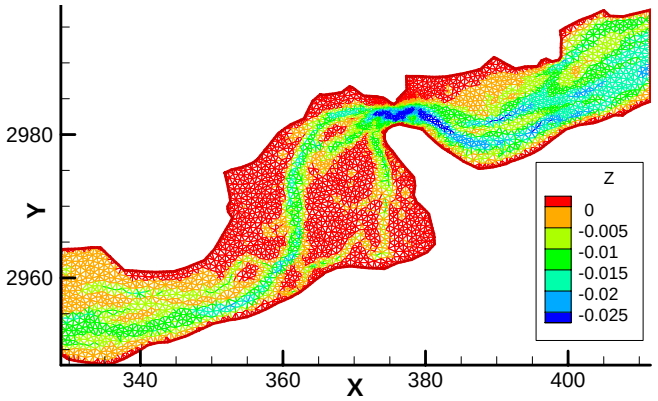

Fig. 7. 2D coloured plane mesh of discrete geometrical model for Qeshm canal (dimension is in km)

The hydrodynamic model calculates the depth-averaged equations in the solving domain. For applying this, the observed data of water level oscillation at the east boundary (SHAHID-RAJAEE Port) and predicted water level oscillation at the west boundary (BASAEED Port) were considered as input data to the numerical domain.

The comparison on water level oscillation results between observed data at KAVEH Pier and numerical model was performed in a period of 24 hours (17-feb-2002) is shown in Fig. 8. It is worth noting that, the velocities comparison between model results and domain gathered data allude to the model competency in tidal currents simulation in the present area. Also, Velocity evaluation on the model outcomes and observed data is shown in Fig. 9.

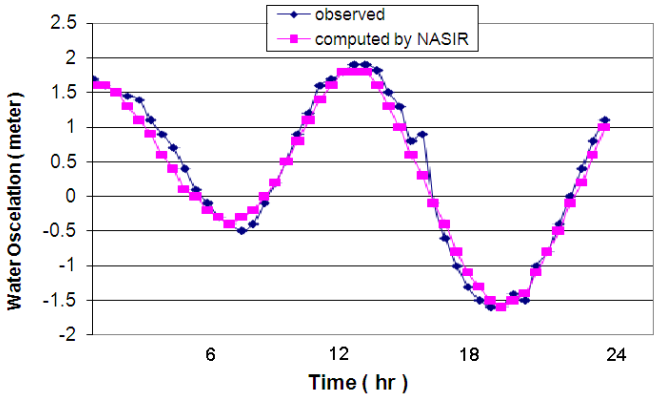

Fig. 8. Curves of water level oscillation obtained from the numerical model and observed data at KAVEH Port in a 24 hours period.

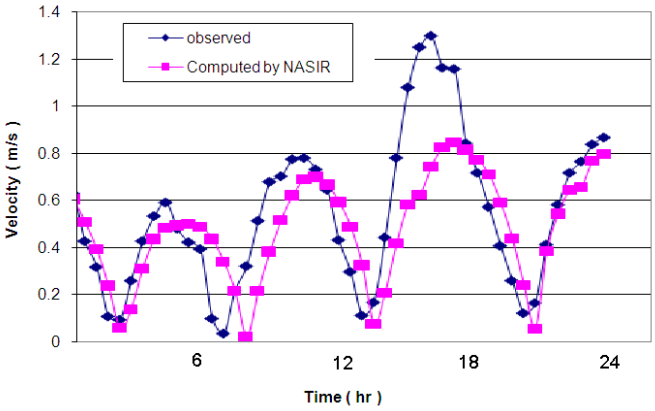

Fig. 9. Curves of flow velocity obtained from the numerical model and observed data at KAVEH Port in a 24 hours period.

The obtained results of the numerical model through the entire domain (the Qeshm canal) are presented after 10*hr* Fig. 10 depicts the results of the flow field of water elevation oscillation by numerical model in 3D form. Also, Fig. 11 and Fig. 12 show velocity contour and velocity vectors in the Qeshm canal after 10*hr*

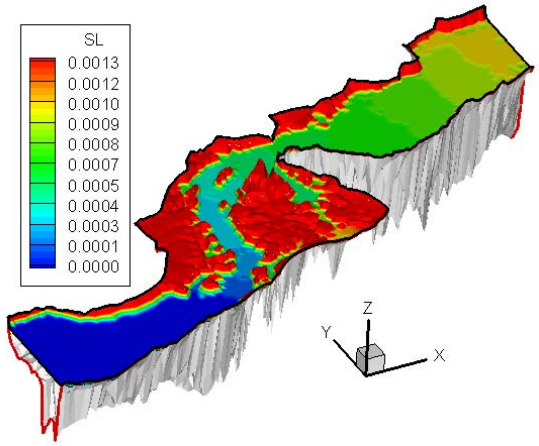

Fig. 10. 3D Colour map of the water elevation alteration (km) in the Qeshm canal (t=10hr)

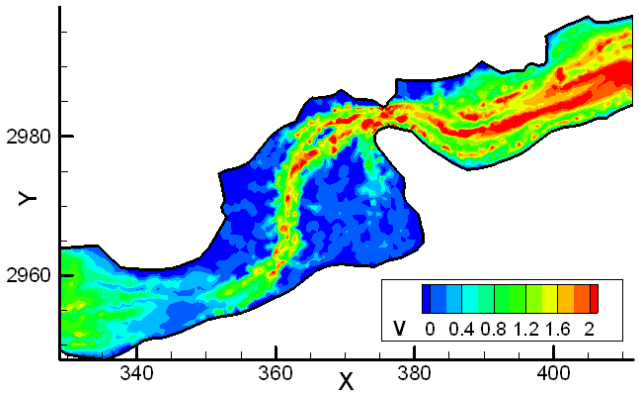

Fig. 11. Map of the velocity coloured contours (km/hr) in the Qeshm canal (t=10hr)

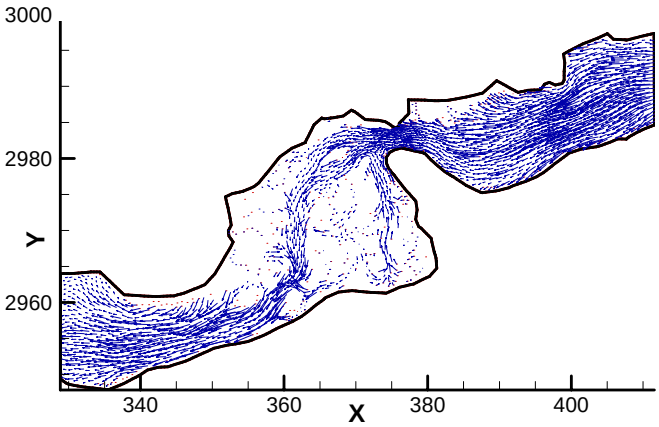

Fig. 12. Demonstration of the velocity vectors (km/hr) in the Qeshm canal (t=10hr)

Results show that the average discrepancy for tidal oscillation between model outcomes and observed data is about 4%. But as it can be seen in Fig. 9, the difference magnitude for velocity is higher than surface water which is about 10%. This could be as a result of measurement inaccuracy or a special effect in the canal.

VIII. Conclusion

The version of NASIR depth average hydrodynamic model simulates the time dependent and circulating problems on variable topography considering wetting and drying areas with reasonable accuracy and considerable efficiency. This model solves the equations of continuity and motions by application of overlapping cell-vertex finite volumes in the form of an unstructured triangular mesh which is converted to a three dimensional surface. Therefore, the geometrical complexities of bed and coastal boundaries variations are efficiently modelled by using unstructured mesh.

By application of an efficient turbulent eddy viscosity model, this software accurately simulates turbulent circulations due to irregularities in the coastal boundaries. This fact is proven by modelling the flow circulations behind a spur dike. The accuracy of the solution results is verified by comparison of the model results with the reported data in the literature.

As a sample application of the developed model to solve flow patterns in a case with irregular variations of bed and coastal boundaries, the tidal currents in the Qeshm canal with wetting and drying Mangrove forests is modelled. The performance and quality of the model are assessed by comparison of the model results with field measurements in a point within the Qeshm canal (Kaveh port). The comparison results on water level surface and velocities, demonstrate the ability and accuracy of the numerical model in simulation of currents the marine canals with geometrically complicated tidal flats.

References

[1] C.B.Vreugdenhil, *Numerical Methods for Shallow water Flow*, Kluwer Academic Publisher, 1994

[2] A. Jameson, T.J. Baker and N.P. Wetherill, "Calculation of InviscidTransonic Flow over a complete Aircraft" , *AIAA Paper*, pp. 1986, pp. 86-0103,

[3] Y. Jia and S.S.Y. Wang, "Numerical Model for Channel Flow and Morphological change Studies", *Journal of Hydraulic Engineering, ASCE.*, vol(125), issue. 9, 1999, pp. 924-933,

[4] R.A. Falconer, P.H. Owens, "Numerical simulation of flooding and drying in a depth-averaged tidal flow model", *Proc. Instn Civ. Engrs*, Part2, pp. 161-180, 1987

[5] W. Wu, "Depth-Averaged Two-Dimensional Numerical Modelling of Unsteady Flow and Non-Uniform Sediment Transport in Open Channels", *Journal of Hydraulic Engineering*, ASCE., vol. 130, issue. 10, 2004, pp. 1013-1024,

[6] *DHI, Water and Environment*, "Modelling the world of water", *Product catalog*, 2005

[7] J.C. Dietrich, R.L. Kolar and R.A. Luettich, *Assessment of ADCIRC's Wetting and Drying Algorithm*, School of Civil Engineering and Environmental Science, University of Oklahoma, Norman, 2004

[8] S.R. Sabbagh-Yazdi, M. Zounemat-Kermani And A. Kermani, "Solution of depth-averaged tidal currents in Persian Gulf on unstructured overlapping finite volumes", *International journal for numerical methods in fluids*, vol. 55, 2007, pp. 81-101,

[9] S.R. Sabbagh-Yazdi and M. Zounemat-Kermani, "Numerical investigation of island effects on depth averaged fluctuating flow in the Persian Gulf", *International Journal of Energy*, Transactions A: Basics Vol. 20, No. 2, 2007, pp. 117-128,

[10] A. Balzan, "Evaluation of methods for numerical simulation of wetting and drying in shallow water flow models", *Coastal Engineering*, vol. 34, 1998, pp. 83–107,

[11] N.P. Weatherill, "A Review of Mesh Generation , Special Lecture", *Advances in Finite Element Technology* , Civil-Compress . Edinbrough, 1996, pp.1-10,

[12] T. Tingsanchali and S. Maheswaran, "2D-Depth-Average flow computation near Groyne", *journal of hydraulic engineering*, ASCE, vol. 116, 1990, pp. 71-86,

[13] J.F. Thompson, B.K. Soni and N.P. Weatherill, *Hand book of grid generation*, CRC Press, New York., 1999

[14] S.R. Massel, K. Furukawa and R.M. Brinkman, "Surface wave propagation in mangrove forests", *Fluid dynamic research*, vol. 24, 1999, pp. 219-249,

[15] J. Struve , R.A. Falconer and Y. Wu, "Influence of model mangrove trees on the hydrodynamics in a flume", *Estuarine, Coastal and Shelf Science*, vol. 58, 2003, pp. 163-171,

[16] Y. Wu , R.A. Falconer and J. Struve, "Mathematical modelling of tidal currents in mangrove forests", *Environmental modelling & Software*, vol. 16, 2001, pp. 19-29,

[17] A. Dissez, D. Sous, S. Vincent, J-P. Caltagirone and A. Sottolichio, "A novel implicit method for coastal hydrodynamics modelling: application to the Arcachon lagoon", *C. R. Mecanique*, vol. 333, 2005, pp. 796–803,

[18] M. Heniche, Y. Secretan, P. Boudreau and M. Leclerc, "A two dimensional finite element drying-wetting shallow water model for rivers and estuaries", *Advances in Water Resources*, vol. 23, 2000, pp. 359-372,

[19] Z.G. Jia, M.R. Morton and J.M. Hamrick, "Wetting and Drying Simulation of Estuarine Processes", *Estuarine, Coastal and Shelf Science*, vol. 53, 2001, pp. 683–700,

[20] M.J. Castro, A.M. Ferreiro, J.A. Garcia-Rodriguez, J.M. Gonzalez Vida, J. Macias, C. Pares and M. ElenaVazquez-Cendon, "The Numerical Treatment of Wet/Dry Fronts in Shallow Flows: Application to One-Layer and Two-Layer Systems", *Mathematical and computer modelling*, vol. 42, 2005, pp. 419-439,

[21] L. Begnudelli and B.F. Sanders, "Unstructured Grid Finite-Volume Algorithm for Shallow-Water Flow and Scalar Transport with Wetting and Drying", *Journal of hydraulic engineering*, vol. 132, 2006, pp. 371-384,

[22] S.F. Bradford and B.F. Sanders, "Finite-volume model for shallow-water flooding of arbitrary topography", *journal of hydraulic engineering*. Vol. 128, 2000, pp. 289–298,